Inorganic Chemistry

Article

pubs.acs.org/IC

Solid State ^{13}C and ^{2}H NMR Investigations of Paramagnetic $[Ni(II)(acac)_2L_2]$ Complexes

Anders Lennartson,† Lene Ulrikke Christensen, Christine J. McKenzie, and Ulla Gro Nielsen*

Department of Physics, Chemistry, and Pharmacy, University of Southern Denmark, Campusvej 55, 5230 Odense M, Denmark

ABSTRACT: Nine structurally related paramagnetic acetylacetonato nickel(II) complexes: $[Ni(acac)_2]$ and *trans*-$[Ni(acac)_2(X)_2]nH/D_2O$, X = H_2O, D_2O, NH_3, MeOH, $PMePh_2$, PMe_2Ph, or $[dppe]_{1/2}$, n = 0 or 1, dppe = 1,2-bis(diphenylphosphino)ethane, as well as *cis*-$[Ni(F_6\text{-}acac)_2(D_2O)_2]$, F_6-acac = hexafluoroacetylonato, have been characterized by solid state ^{13}C MAS NMR spectroscopy. ^{2}H MAS NMR was used to probe the local hydrogen bonding network in $[Ni(acac)_2(D_2O)_2]D_2O$ and *cis*-$[Ni(F_6\text{-}acac)_2(D_2O)_2]$. The complexes serve to benchmark the paramagnetic shift, which can be associated with the resonances of atoms of the coordinated ligands. The methine (CH) and methyl (CH_3) have characteristic combinations of the isotropic shift (δ) and anisotropy parameters (d, η). The size of the anisotropy (d), which is the sum of the chemical shift anisotropy (CSA) and the paramagnetic electron−nuclei dipolar coupling, is much more descriptive than the isotropic shift. Moreover, the CSA is found to constitute up to one-third of the total anisotropy and should be taken into consideration when ^{13}C anisotropies are used for structure determination of paramagnetic materials. The ^{13}C MAS NMR spectra of *trans*-$[Ni(acac)_2(PMe_2Ph)_2]$, *trans*-$[Ni(acac)_2(PMePh_2)_2]$, and the noncrystallographically characterized *trans*-$[Ni(acac)_2(dppe)]_n$ were assigned using these correlations. The complexes with L = H_2O, D_2O, NH_3, and MeOH can be prepared by a series of solid state desorption and sorption reactions. Crystal structures for *trans*-$[Ni(acac)_2(NH_3)_2]$ and *trans*-$[Ni(acac)_2(PMePh_2)_2]$ are reported.

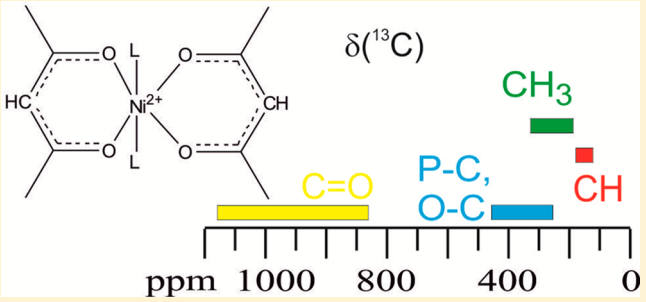

INTRODUCTION

Solid state NMR (SSNMR) spectroscopy is a versatile isotope-selective technique that probes the local environment in materials without requirements of long-range order. Moreover, SSNMR spectra are very sensitive to the magnetic properties, and studies of paramagnetic materials have become accessible with today's SSNMR equipment. Detailed insight into the local environment and magnetic properties of many different paramagnetic materials such as lithium ion batteries,[1] iron soil minerals,[2] amorphous inorganic materials,[3] and paramagnetic proteins[4] has been possible. Ishii et al. have successfully combined solid state ^{13}C NMR techniques with fast MAS to obtain nonbonding metal−carbon distances in $[V(III)(acac)_3]$, $[Mn(III)(acac)_3]$, $[Cu(II)(DL\text{-alanine})_2]$, and $[Cu(II)(glycine)_2]$,[5] as previously achieved for ^{51}V in diamagnetic vanadium compounds in the solid state.[6]

The local environment in nickel complexes can be probed by NMR spectroscopy using one or more of the NMR active isotopes in the ligands (e.g., $^{1,2}H$, ^{13}C, ^{15}N, and ^{31}P) due to the unfavorable properties of the NMR active ^{61}Ni isotope itself (low abundance, quadrupolar, and low-γ nuclei). For paramagnetic inorganic materials ^{2}H NMR is preferred over ^{1}H NMR due to a reduction of the strong electron−nuclear dipolar interaction by a factor of ∼1/6 ($\gamma(^2H)/\gamma(^1H)$), no background signals, and additional structural information from the ^{2}H quadrupole interaction. Diamagnetic Ni(II) complexes have previously been investigated by SSNMR to obtain structural information[7] and monitor single crystal to single crystal transformation.[8] Paramagnetic Ni(II) coordination compounds are much less studied by NMR. Signals are often broadened beyond detection in the liquid state, and only few studies have been reported.[9] A general approach for solids has been to study a diamagnetic analogue.[10] Solid state ^{13}C NMR studies of paramagnetic Ni(II) systems[11] and ^{2}H MAS NMR have given insight into motion and bonding in small paramagnetic $acac^-$ complexes,[12] substrates bound to cytchrome C,[13] metallocenes,[14] and the mobility of the Ni(II) hexaaquo ion.[15]

We have investigated a series of nickel(II) β-diketonato compounds with the general formulation $Ni(acac)_2$ in *trans*-$[Ni(acac)_2(X)_2]nH/D_2O$, X = H_2O, D_2O, NH_3, MeOH, PMe_2Ph, $PMePh_2$, or $[dppe]_{1/2}$, with n = 0 or 1, and *cis*-$[Ni(F_6\text{-}acac)_2(D_2O)_2]$ by solid state ^{13}C MAS NMR spectroscopy (Figure 1). Apart from $[Ni(acac)_2]$ in which only long axial intermolecular interactions of 3.05 Å[16] are present in the solid state, the nickel ions are octahedrally coordinated in these complexes. Our aim was to obtain structural information for these closely related paramagnetic compounds using ^{13}C SSNMR spectroscopy. This work demonstrates paramagnetic solid state NMR spectroscopy in the characterization of

Received: September 17, 2013
Published: December 10, 2013

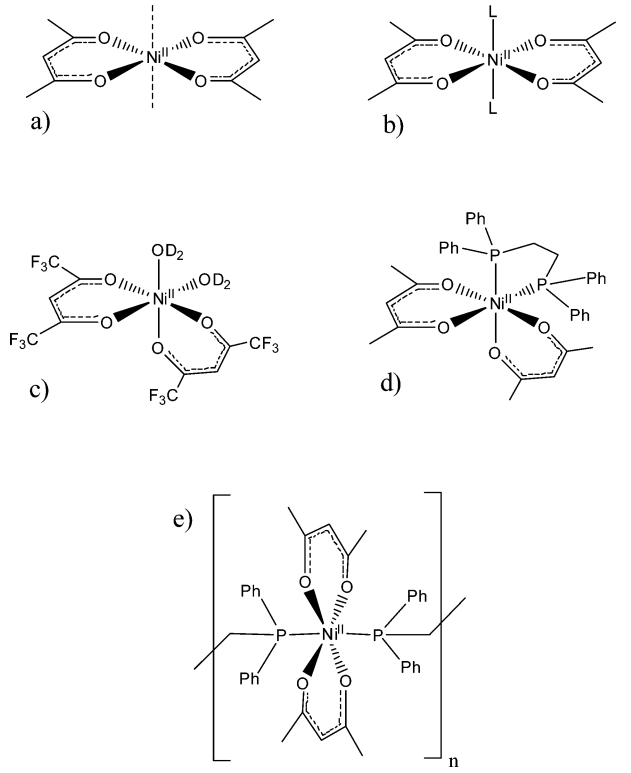

Figure 1. The coordination of Ni(II) in (a) $[Ni(acac)_2]$, (b) *trans*-$[Ni(acac)_2L_2]$ with L = H_2O, D_2O, NH_3, MeOH, PMe_2Ph, and $PMePh_2$, (c) *cis*-$[Ni(F_6\text{-acac})_2(H_2O)_2]$, (d) *cis*-$[Ni(acac)_2(dppe)]$, and (e) polymeric $\{trans\text{-}[Ni(acac)_2(dppe)]\}_n$.

relatively simple nickel coordination compounds with known and unknown crystal structures providing impetus for the use of this technique in the study of more complicated nickel containing materials such as catalysts and enzymes.

EXPERIMENTAL SECTION

Synthesis. *trans*-$[Ni(acac)_2(H_2O)_2](H_2O)$,[17] *trans*-$[Ni(acac)_2]$,[17] and *trans*-$[Ni(acac)_2(PMe_2Ph)_2]$[18] were prepared by published procedures. *cis*-$[Ni(F_6\text{-acac})_2(H_2O)_2]$[19] was recrystallized by dissolution in D_2O/acetone 1:5 to give *cis*-$[Ni(F_6\text{-acac})_2(D_2O)_2]$. $[Ni(acac)_2(D_2O)_2](D_2O)$ was prepared in the same manner as the H_2O complex except D_2O (98% Cambridge Isotope Laboratories) was used as a solvent. Starting materials were purchased from Sigma-Aldrich and were used as received.

[Ni(acac)$_2$]. $[Ni(acac)_2(H_2O)_2](H_2O)$ was heated to 130 °C for 30 min under vacuum. The initially blue crystals gradually changed color to emerald green. Thermogravimetric analysis showed a mass loss corresponding to two water molecules between 60 and 85 °C, followed by the loss of a single water molecule between 85 and 101 °C.

trans-[Ni(acac)$_2$(NH$_3$)$_2$]. A solution of $[Ni(acac)_2]$ (0.50 g, 1.6 mmol) in methanol (100 mL) was filtered and transferred to a 250 mL conical flask, where a small vial containing a few milliliters of aqueous ammonia was hung above the solution, and the flask was sealed. A small hole was punched through the cap of the vial allowing a slow diffusion of ammonia vapor out of the vial. Blue crystalline plates were deposited over 4 days. When the solution was colorless, the mixture was filtered, and the crystals were dried by suction. Yield 0.42 g (90%). Anal. Calcd for $NiC_{10}H_{20}N_2O_4$: C, 41.28; H, 6.93; N, 9.63. Found: C, 40.48; H, 6.88; N, 9.17. IR: 3352 (s), 3273 (m), 3074 (w), 2989 (m), 2921 (w), 1947 (w), 1619 (s), 1515 (s), 1466 (s), 1406 (s), 1243 (s), 1211 (s), 1016 (s), 925 (s), 762 (s), 660 (s), 569 (s) cm^{-1}.

The same material but in powder form was obtained by a simpler gas-diffusion reaction. A beaker with $[Ni(acac)_2]$ was placed inside a jar containing ammonia (25% in water). This jar was sealed and left overnight.

trans-[Ni(acac)$_2$(MeOH)$_2$]. *trans*-$[Ni(acac)_2(MeOH)_2]$ was prepared by gaseous methanol diffusion into a solid sample of $[Ni(acac)_2]$. The purity was confirmed by powder XRD and compared with the reported SC-XRD structure.[20]

trans-[Ni(acac)$_2$(PMePh$_2$)$_2$]. $[Ni(acac)_2]$ (75 mg, 0.3 mmol) was dissolved in 0.25 mL of chloroform, and methyldiphenylphosphine (0.11 mL, 0.6 mmol) was added. $[Ni(acac)_2(PMePh_2)_2]$ crystallized as dark blue crystals overnight. The solution was filtered, and the crystals were dried by suction. Yield: 33 mg (16%). Anal. Calcd for $NiC_{36}H_{40}P_2O_4$: C, 65.78; H, 6.13. Found: C, 65.75; H, 6.17. IR: 3421 (bs), 3054 (m), 2985 (m), 2913 (m), 1588 (s), 1513 (s), 1455 (s), 1435 (s), 1421 (s), 1403 (s), 1357 (m), 1280 (w), 1256 (s), 1194 (s), 1160 (w), 1093 (m), 1016 (s), 921 (s), 895 (s), 884 (s), 859 (w), 761 (s), 754 (s), 742 (s), 722 (m), 698 (s), 678 (w), 653 (w), 619 (w), 575 (m), 502 8s), 481 (m) cm^{-1}.

{trans-[Ni(acac)$_2$(dppe)]}$_n$. $[Ni(acac)_2]$ (102 mg, 0.4 mmol) was dissolved in toluene (3 mL), and the solution was filtered. Ethylenebis-diphenylphosphine (dppe) (159 mg, 0.4 mmol) was added. When a clear solution was obtained, *n*-hexane (4 mL) was added. Within an hour, $\{trans\text{-}[Ni(acac)_2(dppe)]\}_n$ crystallized as light blue microcrystals unsuitable for single crystal XRD. The solution was filtered, and the crystals were dried by suction. Yield: 0.22 g (85%). Anal. Calcd for $NiC_{38}H_{38}P_2O_4$: C, 65.98; H, 5.84. Found: C, 66.34; H, 5.87. IR: 3435 (bs), 3054 (m), 2916 (w), 1588 (s), 1515 (s), 1460 (s), 1434 (s), 1407 (s), 1360 (m), 1257 (m), 1180 (m), 1121 (w), 1103 (w), 1070 (w), 1017 (m), 923 (m), 744 (s), 696 (s), 653 (w), 571 (w), 532 (w), 514 (m), 488 (w) cm^{-1}.

Powder X-ray Diffraction. The sample purity was verified by powder XRD on a Siemens D5000 X-ray diffractometer by scanning 2θ from 4° to 40° in 0.02° steps using Cu K_α (1.5418 Å).

Single Crystal X-ray Crystallography. Diffraction data were collected using a Bruker-Nonius X8 APEX-II instrument (Mo Kα radiation). Structures were solved using SIR-92[21] and refined using SHELXL-97.[22] All non-H atoms were refined anisotropically. A semiempirical absorption correction was applied using the SADABS program. Carbon bonded H atoms were placed in calculated positions and refined using a riding model. Diagrams were drawn using ORTEP-3[23] for Windows. SIR-92, SHELXL, and ORTEP-3 were operated under the WinGX program suit.[24] Details of structure determinations are given in Table 1. CCDC 957466 (*trans*-$[Ni(II)(acac)_2(NH_3)_2]$) and 957467 (*trans*-$[Ni(acac)_2(PMePh_2)_2]$) contain the supplementary crystallographic data for this paper. These data can be obtained free of charge from The Cambridge Crystallographic Data Centre via www.ccdc.cam.ac.uk/data_request/cif.

Solid-State NMR Spectroscopy. ^{13}C and ^{2}H MAS NMR spectra were recorded at 11.7 T on a Varian INOVA 500 MHz instrument using a Chemagnetics 3.2 mm HX MAS NMR probe. The magic-angle was set by minimizing the line width of the ^{79}Br resonances in KBr and ^{2}H resonance in deuterated sodium acetate (CD_3COONa) for ^{13}C and ^{2}H MAS NMR, respectively. ^{13}C and ^{2}H SSNMR spectra are referenced relative to TMS using the CH resonance in adamantane (δ = 38.3 ppm[25]) and D_2O (δ = 4.6 ppm) as secondary references, respectively. Between 10 000 and 100 000 scans were recorded for each spectrum using 0.1 s relaxation delay. Spectra were obtained using different spinning speeds to ensure correct determination of the isotropic resonances. Only small changes in chemical shifts (<2 ppm) due to frictional heating were observed.

NMR Data Analysis. The Varian VnmrJ software and STARS[26] were used for data processing and analysis. The approach of Simonovitch was used to obtain starting parameters for the optimizations.[27] The chemical shift ($\delta = \delta_{iso} + \delta_{fc}$) contains contributions from the isotropic chemical shift and the Fermi-contact shift (δ_{fc}) caused by delocalized unpaired electron density from the Ni(II) ion. The pseudocontact shift is expected to be much smaller than δ_{fc} for the Ni(II) complexes investigated[28] and will not be considered.

The spinning sideband (ssb) patterns in ^{13}C MAS NMR spectra of paramagnetic Ni(II) complexes contains contributions from both the

dx.doi.org/10.1021/ic402354r | Inorg. Chem. 2014, 53, 399−408

Table 1. Crystal and Refinement Data for *trans*-[Ni(acac)$_2$(PMe$_2$Ph)$_2$] and *trans*-[Ni(acac)$_2$(NH$_3$)$_2$]

	[Ni(acac)$_2$(P-MePh$_2$)]	[Ni(acac)$_2$(NH$_3$)$_2$]
empirical formula	$NiC_{36}H_{40}P_2O_4$	$NiC_{10}H_{20}N_2O_4$
M	657.33	290.99
T (K)	150(2)	150(2)
cryst syst	triclinic	monoclinic
space group	$P\bar{1}$	$P2_1/c$
a (Å)	9.0386(4)	10.7620(12)
b (Å)	9.6637(5)	5.4569(5)
c (Å)	10.7038(5)	11.1074(12)
α (deg)	65.924(2)	90
β (deg)	75.175(2)	103.094(5)
γ (deg)	83.526(2)	90
V (Å^3)	825.15(7)	635.35(11)
Z	1	2
D_c (g cm^{-3})	1.323	1.521
μ(Mo Kα) (mm^{-1})	0.722	1.532
cryst size (mm^3)	0.28 × 0.28 × 0.26	0.40 × 0.12 × 0.04
θ range (deg)	3.51−26.03	3.77−25.94
reflns collected	18 941	8486
unique reflns, R_{int}	3199, 0.0209	1235, 0.0435
no. of params	199	93
final $R_1(F)^a$ ($I > 2\sigma(I)$), $wR_2(F^2)^b$	0.0240, 0.0676	0.0443, 0.1175
$R_1{}^a$, $wR_2(F^2)^b$ (all data)	0.0253, 0.0684	0.0572, 0.1301
largest diff. peak and hole (e Å^{-3})	0.323 and −0.239	2.337 and −0.387

$^aR_1(F) = \sum(||F_o| - |F_c||)/\sum|F_o|$. $^bwR_2(F^2) = \{\sum[w(F_o^2 - F_c^2)^2]/\sum[w(F_o^2)^2]\}^{1/2}$.

chemical shift anisotropy (CSA) and electron−dipole interaction. These two tensors have different orientations of their principal axis systems and cannot be separated.[12a] Thus, we report the size and asymmetry of the combined contribution as d and η, respectively, where $d = d_{zz} - \delta$ and $\eta = (d_{xx} - d_{yy})/d$. The ^{2}H NMR spectra are influenced by both the quadrupole interaction, described by the quadrupole coupling constant (C_Q) and asymmetry parameter (η_Q), and the electron−dipole interactions. This results in highly asymmetric spectra from which these can be extracted[12a,13] as discussed in detail for jarosites.[2f] The three Euler angles describing the relative orientation between the quadrupole and electron−dipole tensors could not be determined unambiguously for ^{2}H NMR spectra and are therefore not discussed further.

RESULTS AND DISCUSSION

Syntheses. We have prepared the series of [Ni(acac)$_2$] derived complexes using both wet chemical and solid state techniques. Figure 2 illustrates how the Ni(II) complexes [Ni(acac)$_2$] and *trans*-[Ni(acac)$_2$L$_2$](H$_2$O)$_n$ (L = H$_2$O, D$_2$O, NH$_3$, or MeOH) can be interconverted using desorption and sorption reactions of the solid state of the compounds when the auxiliary ligands are available in gaseous forms. The reversible sorption and desorption of water into [Ni(acac)$_2$] and from *trans*-[Ni(acac)$_2$(H$_2$O)$_2$] is well-known,[29] and the analogous solid state route to a blue compound likely to be *trans*-[Ni(acac)$_2$(NH$_3$)$_2$] was already noted by Ley in 1914.[30] The green [Ni(acac)$_2$] is formed by heating *trans*-[Ni(acac)$_2$(H$_2$O)$_2$](H$_2$O) to 130 °C under vacuum. The resulting product is a polycrystalline emerald green powder. Solid state [Ni(acac)$_2$] is relatively reactive and sorbs gaseous water, methanol, and ammonia over the course of a few hours accompanied by color changes to give *trans*-[Ni(acac)$_2$L$_2$], L = H$_2$O, NH$_3$, or MeOH. *cis*-[Ni(F$_6$-acac)$_2$(D$_2$O)$_2$], *trans*-[Ni(acac)$_2$(PMe$_2$Ph)$_2$], *trans*-[Ni(acac)$_2$(PMePh$_2$)$_2$] and {*trans*-[Ni(acac)$_2$(dppe)]}$_n$ were prepared by more standard solution techniques.

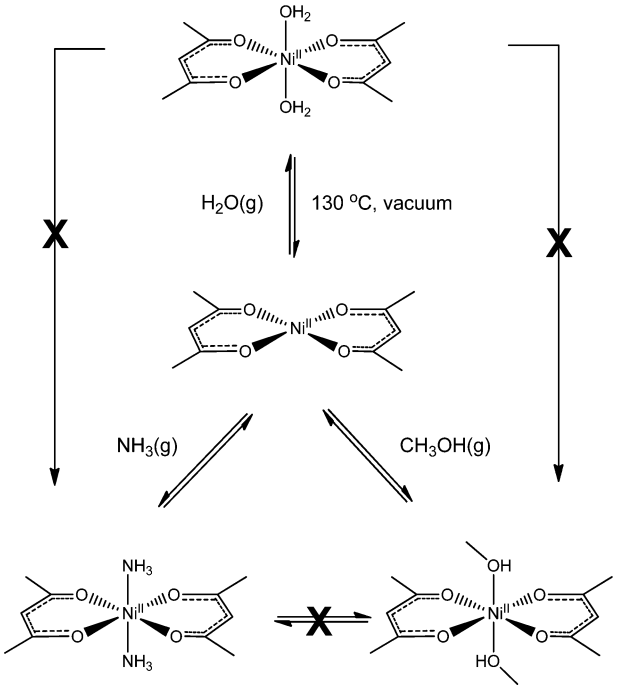

Figure 2. The conversion of *trans*-[Ni(acac)$_2$(H$_2$O)$_2$]H$_2$O to [Ni(acac)$_2$] by heating to 130 °C under vacuum followed by solid−gas phase reactions with ammonia and methanol to form *trans*-[Ni(acac)$_2$(NH$_3$)$_2$] and trans-[Ni(acac)$_2$(MeOH)$_2$], respectively.

X-ray Crystal Structures of *trans*-[Ni(acac)$_2$(NH$_3$)$_2$] and *trans*-[Ni(acac)$_2$(PMePh$_2$)$_2$]. Two of the complexes had not previously been structurally characterized by single crystal X-ray crystallography. Most notably one of these is *trans*-[Ni(acac)$_2$(NH$_3$)$_2$], a compound that has been known for almost a century. Given that *trans*-[Ni(acac)$_2$(NH$_3$)$_2$] is very insoluble, growing crystallography grade crystals proved challenging. For this reason, a slow crystallization method from solution state was devised, and using this we were able to obtain blue plate-like single crystals. The crystal structure of *trans*-[Ni(acac)$_2$(NH$_3$)$_2$], Figure 3a, Table 1, reveals that this is a *trans* compound, similar to the diaquo and dialkoxido analogues. The ammonia ligands are involved in H bonding interactions to acac$^-$ O atoms of adjacent molecules in which the [Ni(acac)$_2$] planes are orientated at 90° with respect to each other. Although these H bonding interactions are not strong (H$_2$N···O2^{i}, 2.51 Å; N$_2$N···O1^{ii}, 2.59; H$_3$N···O1^{iii}, 2.54 Å; symmetry codes (i) x, 1 + y, z; (ii) 2 − x, 1 − y, 2 − z; (iii) x, 1/2 − y, 1/2 + z), there can be two per H atom making for overall strong intermolecular interactions and therewith suggesting a structural reason for the significant insolubility of this compound compared with the other members of this series, except for anhydrous *trans*-[Ni(acac)$_2$(H$_2$O)$_2$]. Thus, it was pertinent to note that *trans*-[Ni(acac)$_2$(NH$_3$)$_2$] is isomorphous with the structure of anhydrous *trans*-[Ni(acac)$_2$(H$_2$O)$_2$] and also contains extensive intermolecular H bonding interactions.[31] The crystal structure of *trans*-[Ni(acac)$_2$(PMePh$_2$)$_2$] also confirms the *trans* arrangement, Figure 3b, Table 1, and is built up by CH···O interactions, involving one of the aromatic *meta* hydrogen atoms, H14 and O2^{i} (symmetry code (iv) 2 − x, −y, 2 − z), with a H14···O2^{iv} distance of 2.4980(18) Å. These hydrogen bonds give rise to chains extended along the

dx.doi.org/10.1021/ic402354r | Inorg. Chem. 2014, 53, 399−408

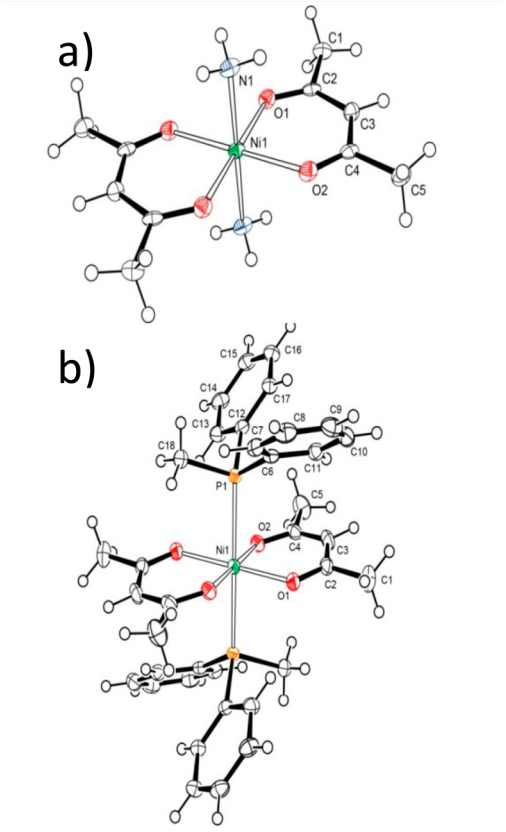

Figure 3. Molecular structures of (a) *trans*-[Ni(acac)$_2$(NH$_3$)$_2$] and (b) *trans*-[Ni((acac)$_2$(PPh$_2$Me)$_2$] displaying the crystallographic numbering schemes. Displacement ellipsoids are drawn at the 50% probability level. Hydrogen atoms are included as spheres of arbitrary radii.

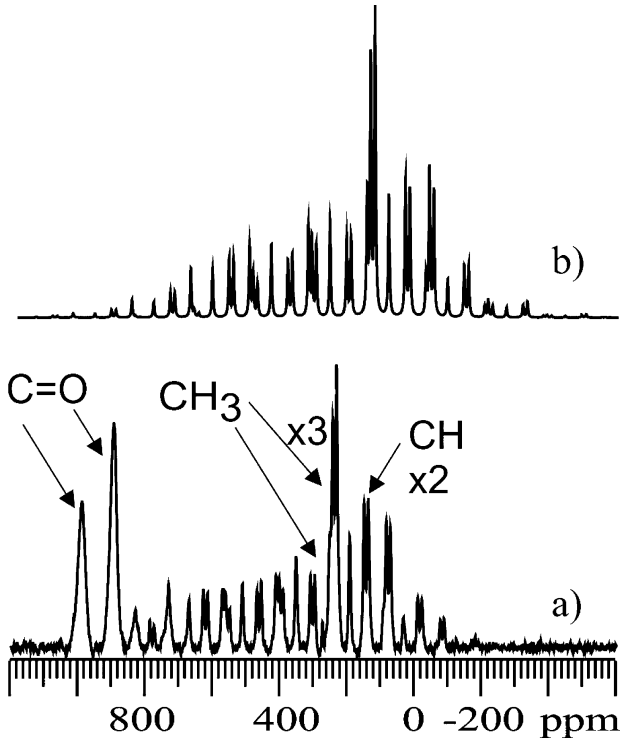

Figure 4. (a) Experimental ^{13}C MAS NMR spectrum of *trans*-[Ni(acac)$_2$(H$_2$O)$_2$]H$_2$O with 18 kHz spinning speed. The isotropic peaks are marked. (b) Simulation of the ^{13}C MAS NMR spectra for CH and CH$_3$ using the parameters in Table 2

crystallographic *a*-axis. The chains are held together by weak dispersion forces, without indications of directed interactions such as hydrogen bonds or $\pi\cdots\pi$ or CH$\cdots\pi$ interactions. A similar set of interactions in *trans*-[Ni(acac)$_2$(PMe$_2$Ph)$_2$] involving *meta* hydrogen atoms and diketonate oxygen atoms give rise to chains along the *a*-axis.[18] The Ni−P distances in *trans*-[Ni(acac)$_2$(PMe$_2$Ph)$_2$] are slightly longer, 2.5004(4) Å, compared with the corresponding distances, 2.4403(5) Å, in *trans*-[Ni(acac)$_2$(PMe$_2$Ph)$_2$]),[17] while the Ni−O distances are identical within a 3σ limit.

Solid State NMR Spectroscopy. *trans-[Ni(acac)$_2$(H$_2$O)$_2$]-(H$_2$O).* The ^{13}C MAS NMR spectrum of *trans*-[Ni(acac)$_2$(H$_2$O)$_2$](H$_2$O) shown in Figure 4 contains the spinning sideband (ssb) manifold from eight ^{13}C resonances. Analysis of these ssbs yields information about the isotropic shift (δ(^{13}C)) and the anisotropy (*d*, η) (Table 2). δ(^{13}C) reflects the proximity to the paramagnetic center via the chemical bonds, while *d* and η contains information about the distance to the paramagnetic centers and, as a smaller but not necessarily negligible contribution, the chemical shift anisotropy (CSA), that is, the symmetry of the electron distribution around ^{13}C.

The ^{13}C NMR resonances fall within three chemical shift regions, δ > 900 ppm (2), $\delta \approx$ 120−140 ppm (2), and $\delta \approx$ 180−310 ppm (4), where the number of resonances in each region is given in parentheses. Ten ^{13}C resonances from the two crystallographically inequivalent acac$^-$ ligands are expected based on the reported crystal structure for this compound.[32] The two peaks with δ > 900 ppm are severely broadened due to close proximity to the paramagnetic Ni(II) ion and contain the four carbonyl resonances, which pairwise must have chemical shift difference smaller than the line width. Assignment of the other resonances is less obvious because paramagnetic shifts can be both positive and negative moving the ^{13}C shift, δ(^{13}C), away from the diamagnetic fingerprint value.

Analysis of the ssb patterns, summarized in Table 2, shows that the parameters for the isotropic shift (δ), the anisotropy (*d*), and the asymmetry parameter (η) fall in two categories. The two resonances at 124 and 136 ppm are characterized by *d* < 350 ppm, whereas the remaining four resonances (δ = 188, 201, 245, and 311 ppm) have 180 < δ < 310 and *d* > 450 ppm. The crystallographic unit cell contains twice as many CH$_3$ as CH in the asymmetric unit.[32] Thus, the two resonances at 120 and 136 ppm are assigned to methine (^{13}CH) and the remaining resonances to the methyl groups (^{13}CH$_3$). The NMR parameters for two methines are very similar, whereas the local environments for the methyl groups exhibit a much larger structural variation. This is expected since the O═C−CH═CO moiety is rigid and shows very little structural variation in the compounds investigated. Moreover, the Me groups are closer to Ni(II) in neighboring complexes.

We can extract more information when we compare the data in Table 2 to those previously reported. The contribution from the paramagnetic (Fermi-contact, δ_{fc}) shift to the isotropic shift can be estimated based on δ_{iso}(^{13}C) reported earlier in literature for structurally related compounds. Earlier, less detailed liquid state ^{13}C NMR studies of weakly paramagnetic tetrahedral Ni(II) β-imino carbonyl enolate complexes detected δ_{iso} = 24.7−30.0 ppm and 181.2−187.4 for CH$_3$ and C═O, respectively.[11a] The value for β-C (CH) was higher due to substitution at this position and cannot be compared directly with our samples.[11a,b] A recent detailed solid state NMR and

dx.doi.org/10.1021/ic402354r | Inorg. Chem. 2014, 53, 399−408

Table 2. ^{13}C NMR Parameters Determined for *trans*-[Ni(acac)$_2$L$_2$] with L = H$_2$O, D$_2$O, NH$_3$, and MeOH and *trans*-[Ni(F$_6$-acac)$_2$]

compound	group	δ (ppm)	d (ppm)	η_d	comments
trans-[Ni(acac)$_2$(H$_2$O)$_2$](H$_2$O)	CH$_3$	188(1)	−567(13)	0.55(5)	one molecule[32]
		201(1)	−605(10)	0.41(10)	
		245(1)	−496(10)	0.60(8)	
		311(2)	−625(15)	0.67(7)	
	CH	124(1)	−310(20)	0.30 (5)	
		136(1)	−348(20)	0.37(13)	
	C═O	950(20)	%[a]	%	
		1020(20)	%	%	
trans-[Ni(acac)$_2$(D$_2$O)$_2$](D$_2$O)	CH$_3$	188(1)	−567(13)	0.55(5)	one molecule
		201(1)	−605(10)	0.5(1)	
		244(1)	−496(10)	0.52(7)	
		303(2)	−625(15)	0.70(5)	
	CH	124(1)	−337(12)	0.3(1)	
		135(1)	−380(17)	0.2(2)	
	C═O	940(10)	%	%	
		1027(10)	%	%	
[Ni(acac)$_2$]	CH$_3$	174(1)	−565(40)	0.55(10)	
	CH	132(1)	−313(8)	0.10(10)	
	C═O	850(20)	%	%	
		900(20)	%	%	
trans-[Ni(acac)$_2$(NH$_3$)$_2$]	CH$_3$	199(1)	−505(5)	0.67(5)	1/4 molecule
	CH	119(5)	−353(7)	0.00(5)	(This work)
	C═O	900(30)	%	%	
trans-[Ni(acac)$_2$(MeOH)$_2$]	CH$_3$	190(1)	−600(50)	0.45(15)	1/2 molecule[20]
		203(2)	−587(60)	0.5(1)	
	CH	138(1)	−360(50)	0.2(2)	
	C═O	797(15)	%	%	
	MeOH	882(20)	%	%	
		245(2)	%	%	
cis-[Ni(F$_6$-acac)$_2$(D$_2$O)$_2$]	CF$_3$	262(2)	−557(23)	0.25(25)	one molecule
		281(2)	−567(33)	0.15(15)	
		292(2)	−620(30)	0.15(15)	
	CH	123(1)	−292(22)	1.00(5)	
		139(1)	−355(15)	0.50(5)	
	C═O	1150(30)	%	%	

[a]% This parameter could not be determined.

DFT study of [Al(III)(acac)$_3$] will be used as reference values for the diamagnetic shifts.[33] Values of $\delta_{iso}(^{13}C)$ = 189−191 ppm (CO), 99−103 ppm (CH), and 26−28 ppm (CH$_3$) were reported.[33] Comparing the two sets of data, we see that the diamagnetic isotropic chemical shifts for the three sites in an acac$^-$ complex are $\delta_{iso}(^{13}C)$ = 185(6) ppm (CO), 101(4) ppm (CH), and 26(5) ppm (CH$_3$). We use this average value to estimate δ_{fc} at 750−830 ppm (CO), 25−35 ppm (CH), and 160−300 ppm (CH$_3$) for *trans*-[Ni(acac)$_2$(H$_2$O)$_2$](H$_2$O). The anisotropy contains contributions from both the chemical shielding tensor and the electron−nuclear dipole interaction. Again we use the diamagnetic [Al(III)(acac)$_3$] for which the reported chemical shift anisotropies (CSA) are approximately −115 ppm (CO), 107 ppm (CH), and 18 ppm (CH$_3$).[34] The ^{13}C CSA for the Ni(II) complex is expected to be very similar. Comparing the total anisotropies determined (Table 2), we see that for the methine the CSA (ca. 107 ppm) constitutes a significant part of the total anisotropy (−348 to −310 ppm) whereas for the methyls the contribution is negligible (ca. 20 ppm CSA vs −500+ ppm). Thus, the use of anisotropies determined from ^{13}C SSNMR for distance determination should be done with caution. The ^{13}C MAS NMR data for the deuterated analogue, *trans*-[Ni(acac)$_2$(D$_2$O)$_2$](D$_2$O), are identical within the error limits (Table 2); these will therefore not be discussed separately.

[Ni(acac)$_2$]. The ^{13}C MAS NMR spectrum (Figure 5) is surprisingly simple with only four resonances, implying a single phase product with a well-defined local environment. Table 2 summarizes the NMR parameters determined from analysis of the spectra. Two peaks of comparable intensity are observed at δ = 850(20) and 900(20) ppm, in the region for a carbonyl isotropic shift suggesting the presence of one acac$^-$ ligand in the asymmetric unit. The two resonances at δ_{iso} = 132 and 174 ppm are assigned to CH and CH$_3$, respectively. The paramagnetic shifts observed in the ^{13}C MAS NMR confirm that the acac$^-$ is still coordinated to Ni(II) and both the crystal and coordinated water have been lost upon heating. Two structures with a Ni(II)/(acac$^-$) ratio of 1:2 have been reported in the literature, a monomer ([Ni(acac)$_2$])[35] and a trimer ([Ni$_3$(acac)$_6$]).[29,36] ^{13}C MAS NMR shows that our compound is the monomer since the reported single-crystal XRD structure of the trimer implies 30 ^{13}C NMR resonances.[29,36] Moreover, rearrangement, with requisite concomitant bond cleavage and formation, from a monomeric (*trans*-[Ni(acac)$_2$(H$_2$O)$_2$]-

dx.doi.org/10.1021/ic402354r | Inorg. Chem. 2014, 53, 399−408

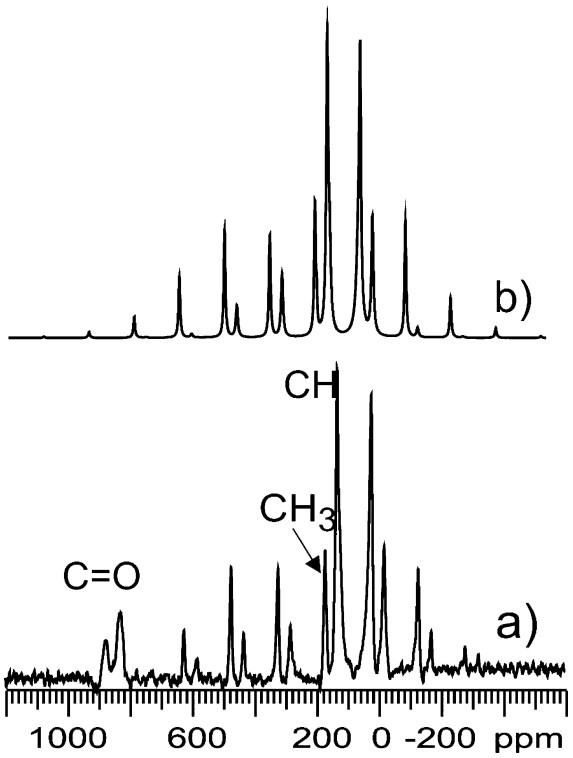

Figure 5. (a) Experimental ^{13}C MAS NMR spectrum of $[Ni(acac)_2]$ using 18 kHz spinning speed. The positions of the isotropic resonances are marked. (b) A simulation of CH and CH_3 using the parameters in Table 2.

(H_2O)) to a trimer upon loss of coordinating ligand and crystal water in a solid state reaction would seem highly unlikely. Thus, ^{13}C MAS NMR shows a well-defined, noncrystalline product with the molecular formula $[Ni(acac)_2]$ illustrating the applicability of SSNMR to probe the local structure in noncrystalline, paramagnetic materials.

trans-[Ni(acac)$_2$(NH$_3$)$_2$]. The molecules of *trans*-$[Ni(acac)_2(NH_3)_2]$ are located on crystallographic inversion centers; thus the asymmetric unit consists of a half molecule. Closer inspection of the hydrogen bonding scheme reveals pseudosymmetry suggesting that only 1/4 molecule should be seen in the solid state NMR spectrum (Table 1 and Figure 3a). In agreement with the crystal structure, the ^{13}C MAS NMR spectrum of *trans*-$[Ni(acac)_2(NH_3)_2]$ in Figure 6 is very simple and contains only the ssb manifolds from the three resonances with δ = 900(30), 199(1), and 119(1) ppm (Table 2), which are assigned to CO, CH_3, and CH, respectively, using the shift anisotropies.

trans-[Ni(acac)$_2$(MeOH)$_2$]. Five resonances from the single $acac^-$ ligand and one from the single MeOH group in the crystal structure are detected by solid state ^{13}C MAS NMR and have been assigned using the isotropic shifts and anisotropies (Table 2). The MeOH resonances at δ = 245 ppm is only two bonds away from the Ni(II) center like the $^{13}C{=}O$ and is broader than CH and CH_3. The anisotropy could not be determined for the MeOH resonance.

cis-[Ni(F$_6$-acac)$_2$(D$_2$O)$_2$]. By contrast to the other complexes in the series, this complex shows a *cis* arrangement of the water ligands and the Ni(II) ion and the carbon atoms of the two F_6-acac ligands are no longer coplanar (Figure 1c). Several overlapping resonances were observed in the ^{13}C MAS NMR

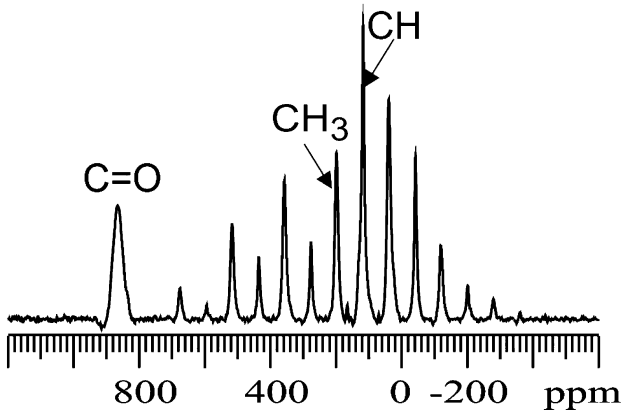

Figure 6. ^{13}C MAS NMR spectrum of *trans*-$[Ni(acac)_2(NH_3)_2]$ using 20 kHz spinning speed. The positions of the isotropic resonances are marked.

spectra at all spinning speeds, and the anisotropy parameters (Table 2) could only be estimated based on visual comparison of experimental and simulated spectra resulting in less precise determination of the anisotropic interaction parameters. However, a clear distinction between C=O, CH, and CF_3 groups is possible based on both δ and d (Table 2). $\delta(^{13}C)$ for the CF_3 group is significantly higher than that for the CH_3 groups in the other compounds reflecting the electronegativity of fluorine.

Summary of ^{13}C NMR Parameters for the acac$^-$ Ligand in the Ni-Complexes. A plot of the anisotropy (δ) as a function of the isotropic shift (Figure 7) clearly shows that CH and CH_3 groups can be distinguished based on their (δ, d) values. CH groups are characterized by $100 < \delta < 150$ ppm and $-400 < d < -300$ ppm, whereas CH_3 fall within $185 < \delta < 300$ ppm and $-650 < d < -500$ ppm in this series of Ni(II) acac complexes.

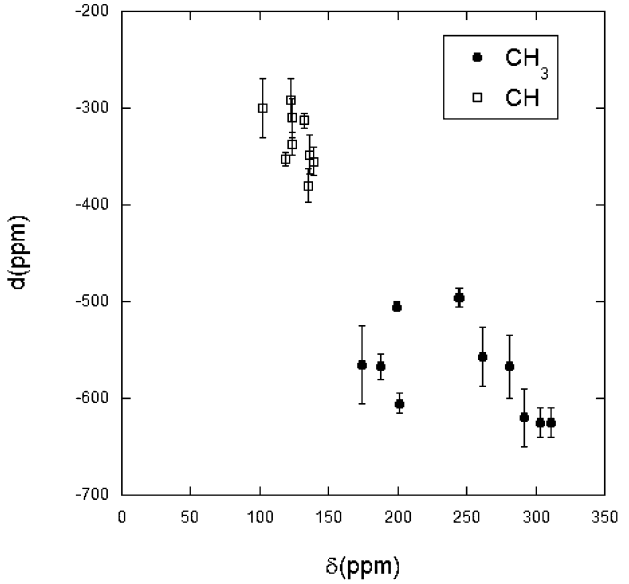

Figure 7. Plot of ^{13}C NMR interaction parameters (δ, d) for the $-CH_3$ and $-CH$ groups of the $acac^-$ ligand. This clearly shows that these two groups can be distinguished by ^{13}C NMR. The sign of the dipole anisotropy is uncertain for *cis*-$[Ni(F_6\text{-acac})_2(H_2O)_2]$; we have assumed this to be negative given the observation for the other $acac^-$ complexes.

dx.doi.org/10.1021/ic402354r | *Inorg. Chem.* 2014, 53, 399−408

Thus, the anisotropy appears more indicative of the local structure than the isotropic shift. Moreover, the CH moiety shows the least variation reflecting that the geometry of the conjugated system is almost identical in all systems. Equipped with this correlation between structure and ^{13}C NMR parameters, we now present and interpret the ^{13}C MAS NMR spectra of three phosphine complexes.

Phosphines. *trans*-[Ni(acac)$_2$(PMe$_2$Ph)$_2$] and *trans*-[Ni(acac)$_2$(PMePh$_2$)$_2$] will be discussed first, because they structurally are very similar differing only in the relative number of Me and Ph substituents in the phosphine ligand. Because of the presence of ten or more resonances, complicated ^{13}C NMR spectra are obtained (Figure 8a,b) and only the isotropic shifts could be determined (Table 3).

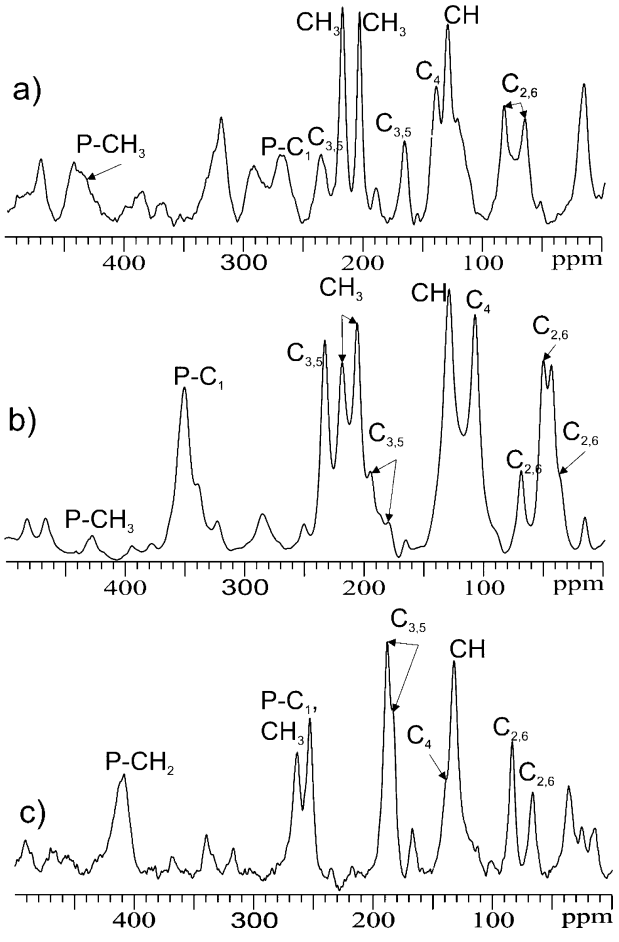

Figure 8. The isotropic region of the ^{13}C MAS NMR spectra of (a) *trans*-[Ni(acac)$_2$(PMe$_2$Ph)$_2$] (19 kHz), (b) *trans*-[Ni(acac)$_2$(PMePh$_2$)$_2$] (20 kHz), and (c) {*trans*[Ni(acac)$_2$(dppe)]}$_n$ (18 kHz). Note that the region for the carbonyl shifts is not shown. The isotropic resonances are indicated; all other resonances are spinning side bands.

trans-[Ni(acac)$_2$(PMe$_2$Ph)$_2$]. The ^{13}C MAS NMR spectrum contains 11 different resonances in the region from 20 to 950 ppm. Thirteen ^{13}C NMR resonances are expected based on the reported crystal structure of this compound.[18] In the carbonyl region, the single, broad resonance at δ = 950(20) ppm is readily assigned to C═O in the acac$^-$ ligand. Two resonances at δ = 207 and 220 ppm are assigned CH_3 in the acac$^-$ ligand. This assignment is further supported by the observation of two resonances at δ = 206(1) and 220(1) ppm in the spectrum of

Table 3. ^{13}C NMR Chemical Shifts of *trans*-[Ni(acac)$_2$(X)$_2$], X = P-Me$_2$Ph and P-MePh$_2$[a]

compound	group	δ (ppm)	^{13}C in asymmetric unit
trans-[Ni(acac)$_2$(PMe$_2$Ph)$_2$]	$C_{2,6}$	68(1), 84(1)	1/2 molecule[18]
	CH	131(2)	
	C_4	141(2)	
	$C_{3,5}$	168(1), 239(2)	13 ^{13}C
	CH_3	207(1), 220(1)	
	P−C_1	271(2)	
	P-Me	431(2)	
	C═O	950(30)	
trans-[Ni(acac)$_2$(PMePh$_2$)$_2$]	$C_{2,6}$	20(3), 38(1), 52(3)	1/2 molecule
	C_4	110(1)	
	CH	131(1)	18 ^{13}C
	$C_{3,5}$	197(3), 185(3), 233(1)	
	CH_3	206(1), 219(1)	
	P−C_1	348(1)	
	P-Me	425(1)	
	C═O	950(10), 814(10)	
{*trans*-[Ni(acac)$_2$(dppe)]}$_n$	$C_{2,6}$	64, 82	1/4 molecule
	CH	130(2)	10 ^{13}C
	C_4	136(2)	
	$C_{3,5}$	182(2), 185(2)	
	P−C_1, CH_3	251(2), 263(2)	
	P-CH_2	410(3)	
	C═O	926(20)	

[a]For ^{13}C in the phosphine ligands, CH_2 refer to CH_2 in dppe, Me and C_i to Me and carbon the phenyl groups coordinated to P, respectively.

trans-[Ni(acac)$_2$(PMePh$_2$)$_2$] (Figure 8b). There are two peaks at δ = 131 and 141 ppm in the isotropic shift region for methine (CH) in the acac$^-$ ligand, and only one is expected based on the reported crystal structure.[18] The resonance with δ = 131(1) ppm is assigned to CH since because it is observed in the ^{13}C NMR spectra of all three phosphine complexes (Table 3 and Figure 8). The peak at δ = 431 ppm has the largest isotropic shift, apart from the readily distinguished C═O, and shows a paramagnetic broadening larger than that observed for the acac-derived CH and CH_3 groups. This ^{13}C must be two bonds away from Ni(II) and belong to either P−C1, the quaternary aromatic carbon from the unique phenyl, or P-Me, the two methyl groups in the phosphine. In the closely related *trans*-[Ni(acac)$_2$(PMePh$_2$)$_2$], two peaks are observed at 425 and 348 ppm. By comparison the ^{13}C MAS NMR spectra of *trans*-[Ni(acac)$_2$(PMe$_2$Ph)$_2$] (Figure 8a) and *trans*-[Ni(acac)$_2$(PMePh$_2$)$_2$] (Figure 8b), we see that the relative intensity of these peaks and each peak relative to the unique CH(acac$^-$) at 131 ppm change. The intensity of the δ = 431 ppm peak is lower in Figure 8b compared with Figure 8a, whereas that of the 348 ppm peak shifts to 271 ppm and doubles in intensity. Thus, we assign the resonance at 431 ppm to two P−Me groups in the asymmetric unit, their isotropic shifts being equivalent. The resonance at 271 ppm is the quaternary carbon in the benzene ring, P−C_1. That a larger shift is observed for the Me groups fits well with the observation that Me groups in the acac$^-$ ligand experience larger paramagnetic shifts than the methine; δ = 68, 84, 141, 168, and 239 ppm belong to the remaining five aromatic carbons in the phosphine ligand. The phenyl is a conjugated

dx.doi.org/10.1021/ic402354r | Inorg. Chem. 2014, 53, 399−408

system with delocalized electrons for which alternating positive−negative−positive−negative paramagnetic shifts decrease in magnitude with the number of bonds from paramagnetic.[9b] Thus, for C_2 and C_6, a large negative shift is expected, for C_3 and C_4 a positive shift, and finally, C_3, which is furthest away, should have small, positive paramagnetic shift. We assign δ = 68 and 84 ppm to two ortho carbons (C_2 and C_6), 168 and 239 ppm to two meta (C_3 and C_5), and 141 ppm to C_3. Further assignment cannot be made based on the current data.

trans-[Ni(acac)$_2$(PMePh$_2$)$_2$]. The structure of this complex contains half a molecule, that is, one acac$^-$ ligand, two phenyl groups, and one methyl group in the asymmetric unit resulting in 18 crystallographically inequivalent ^{13}C (Table 3). The assignment (Table 3) was performed as outlined above.

trans-[Ni(acac)$_2$(dppe)]. The compound was synthesized to have on hand a *cis*-diphosphine complex since it can be reasonably expected that the chelate effect pertaining to dppe would impose the *cis*-[Ni(acac)$_2$(dppe)] structure. Thus, in contrast to expectations, the ^{13}C MAS NMR is surprisingly simple compared with the two other phosphine complexes and for a complex with 36 carbons per molecular unit. Only 10 well-resolved resonances are observed; nine are shown in Figure 8c and the tenth is in the C═O region. The presence of 10 resonances implies a high degree of local symmetry, reminiscent of the spectra recorded for[Ni(acac)$_2$] and *trans*-[Ni(acac)$_2$(NH$_3$)$_2$]. In analogy to these compounds, we propose that the asymmetric unit contains one-quarter of a molecule (C═O, CH, CH$_3$, P−CH$_2$, and the six C's in the unique phenyl group) resulting in 10 inequivalent ^{13}C (Table 3).

The two resonances at 251(2) and 263(2) originate from CH$_3$ and P−C$_1$, but further assignment is not possible The dppe ligand is well-known to bridge between metal ions, sometimes forming 1D polymers.[37] Formulation of our dppe adduct of [Ni(acac)$_2$] as the coordination polymer {*trans*-[Ni(acac)$_2$(μ_2-dppe)]}$_n$ would satisfy the requirement of high symmetry suggested by the NMR spectra.

^{2}H MAS NMR Spectroscopy. ^{2}H SSNMR spectroscopy was used to gain insight into the local hydrogen network for *cis*-[Ni(F$_6$-acac)$_2$(D$_2$O)$_2$] and *trans*-[(Ni(acac)$_2$(D$_2$O)$_2$]D$_2$O.

cis-[Ni(F$_6$-acac)$_2$(D$_2$O)$_2$]. The ^{2}H NMR spectrum of *cis*-[Ni(F$_6$-acac)$_2$(D$_2$O)$_2$] consists of a single ^{2}H site with δ_{iso}(^{2}H) = 52(1) ppm, as illustrated in Figure 9. Both the ^{2}H quadrupole coupling and the paramagnetic dipole interaction caused by the unpaired electrons on Ni(II) contribute to the spectrum resulting in a highly asymmetric pattern. The reduced quadrupole coupling constant, C_Q, of 117(10) kHz and η_Q = 0.65(10) implies that the water molecule is rotating rapidly around the Ni−O bond axis thereby making the two crystallographically inequivalent deuterons[38] magnetically equivalent on the time scale of ^{2}H MAS NMR, a common observation for non-hydrogen bound coordinated water molecules in ^{2}H SSNMR at room temperature.[39] This high mobility is in agreement with the crystal structure, which only shows weak hydrogen bonding possibilities.[40] The strong paramagnetic dipole interaction of −574(10) ppm reflects that the water molecule is in close proximity to Ni(II) and an orbital with unpaired electrons.

trans-[Ni(acac)$_2$(D$_2$O)$_2$](D$_2$O). The ^{2}H MAS NMR spectrum shown in Figure 10a is more complicated than that of *cis*-[Ni(F$_6$-acac)$_2$(D$_2$O)$_2$] and shows the ssb patters from two group of resonances, a site with δ = −11 ppm and a broad

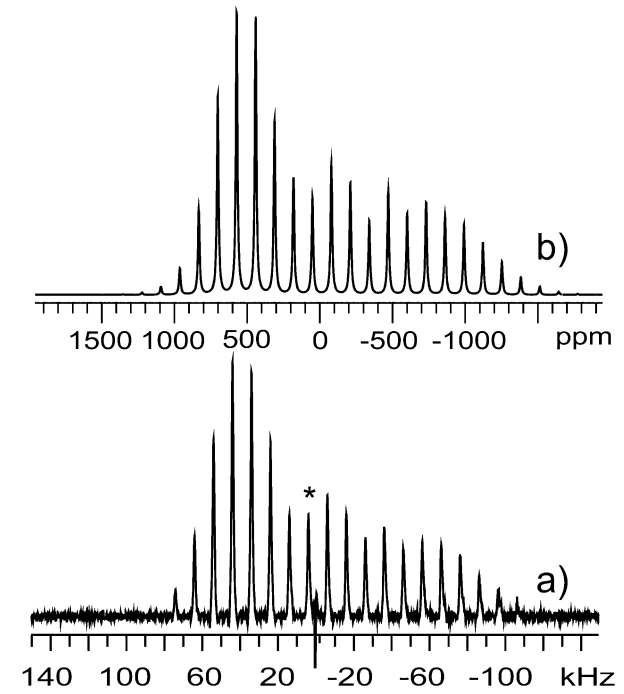

Figure 9. (a) Experimental ^{2}H NMR spectrum of *cis*-[Ni(F$_6$-acac)$_2$(D$_2$O)$_2$] using 10 kHz spinning speed. The asterisk indicates the position of the isotropic resonances. (b) Simulation using the parameters listed in Table 4.

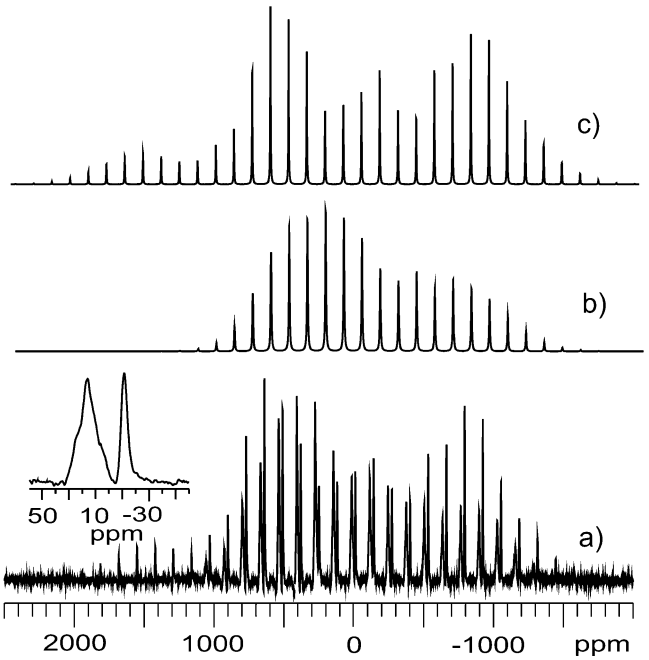

Figure 10. Experimental ^{2}H MAS NMR spectrum of *trans*-[Ni(acac)$_2$(D$_2$O)$_2$]D$_2$O using 10 kHz spinning speed. The inset is an expansion of the regions for the isotropic chemical shifts. (b) Simulation of the resonances with δ(^{2}H) = −11 ppm and (c) the three sites with δ(^{2}H) = 6−25 ppm using the parameters in Table 4

resonance containing three overlapping resonances with $\delta_{iso} \approx$ 6, 17, and 25 ppm and an approximately 1:2:1 intensity ratio (Inset Figure 10a). The site with δ = −11 ppm can be analyzed in detail, whereas only a set of "average" parameters was obtained for the three resonances in the region δ = 6−25 ppm

dx.doi.org/10.1021/ic402354r | Inorg. Chem. 2014, 53, 399−408

Table 4. ^{2}H NMR Parameters for the Deuterated Complexes *cis*-[Ni(F_6-acac)$_2$(D_2O)$_2$] and *trans*-[Ni(acac)$_2$(D_2O)$_2$](D_2O), as Determined from Least-Squares Fitting to the Integrated Spinning Sideband Intensities

compound		C_Q (kHz)	η_Q	d (ppm)	η_D	δ (^{2}H) (ppm)
cis-[Ni(F_6-acac)$_2$(D_2O)$_2$]		117(5)	0.65(5)	−574(10)	0.35(5)	52(1)
trans-[Ni(acac)$_2$(D_2O)$_2$](D_2O)	-CD	185(2)	0.02(5)	−245(50)	0.85(5)	−11(1)
	-Ni−OD_2[a]	115(10)	0.65(5)	−600(50)	0.8(1)	25(1), 17(1)6(1)

[a]The resonance consists of three overlapping sites, and the parameters reported are the average obtained from analysis of the integrated ssb intensities. The relative intensity of these site is approximately 1:2:1 (δ = 17(1) ppm is the most intense).

(Table 4). Close inspection of the line shape for the individual ssbs shows that the 1:2:1 intensity ratio is maintained, that is, these sites all have very similar ^{2}H NMR parameters. The site with δ = −11 ppm has ^{2}H quadrupole coupling parameters characteristic for a deuteron rigid on the NMR time scale and is assigned to CD in the acac$^-$ ligand based on earlier liquid state NMR studies.[41] Exchange of the acidic methine proton is not uncommon and has been reported earlier for M(acac)$_3$ (M = V(III), Mn(III), Al(III), and Co(II)) complexes.[12b,42] The two crystallographically inequivalent methine protons are identical within the resolution of our ^{2}H NMR spectra. Table 4 shows that the three resonances in the 6−25 ppm region have values characteristic for water molecules performing rapid C_2 flips making the two deuterons equivalent on the NMR time scale at room temperature. There are two unique water molecules directly coordinated to Ni(II) with similar Ni−OH_2 distances (2.073 and 2.076 Å) and Ni−O−H angles are between 103° and 113°.[32] The O−H···O_W distances are 2.78−2.80 Å, which are fairly weak hydrogen bonds. ^{2}H MAS NMR shows that these three deuterons are mobile on the NMR time scale at room temperature. The crystallographic water molecule is disordered, and therefore actual bond lengths and angles for this water are unknown. It most likely forms hydrogen bonds with the Ni−OD_2 groups and the C═O. The crystal water is furthest away from Ni(II) and is expected to show the smallest paramagnetic shift. Thus, the site with δ = 6 ppm is the crystal water. To distinguish the two water ligands, we look at the Ni−O−D bond angles, which are 107.3° and 110.6°, due to the rapid rotation of the water ligands. Paramagnetic shifts are very sensitive to the Ni−O−D bond angle, the closer the value is to 90°, the larger paramagnetic shift is expected.[1] We assign the Ni−OD_2 with the largest average Ni−O−D bond angle of 107.3° to the site at δ = 25 ppm and the other Ni−OD_2 at δ = 17 ppm.

CONCLUSIONS

Solid state ^{13}C and ^{2}H NMR spectroscopy has given insight into the local environment in a series of paramagnetic [Ni(acac)$_2$]-derived complexes. This included the series of [Ni(acac)$_2$] and *trans*-[Ni(acac)$_2L_2$] with L = H_2O, NH_3, and MeOH, which are related by a series of solid−gas phase reactions. Correlation between the NMR parameters (δ, d, and η) and the chemical environment was established based on the study of these complexes and the substituted diastereomer *cis*-[Ni(F_6-acac)$_2$(D_2O)$_2$]. The works also revealed that the CSA constitutes up to half the size of the paramagnetic dipolar interaction. Thus, the contribution from the CSA should be taken into account when anisotropies are used for calculation of distances to paramagnetic centers and structure determination.

Solid state gas phase reactions with powder samples intermediates have been characterized using solid state ^{13}C NMR. Moreover, the more complex ^{13}C MAS NMR spectra of three phosphines, ([Ni(acac)$_2L_2$], L = PMe_2Ph and $PMePh_2$ and dppe$_{1/2}$), which have 10−18 ^{13}C resonances, were assigned using isotropic shift correlations established.

Solid state ^{13}C MAS NMR revealed a high degree of symmetry in the coordination environment of the dppe complex suggesting that the compound is a coordination polymer.

The current work demonstrates the application of SSNMR for characterization of paramagnetic disordered materials, complex systems, and natural samples potentially with low concentrations of the compound of interest; assignment based on chemical shifts and dipole interaction is more feasible than determination of relaxations times. In addition, no *a priori* knowledge of interatomic distances is required.

AUTHOR INFORMATION

Corresponding Author

*E-mail: ugn@sdu.dk. Phone: +45 6550 4401.

Present Address

[†]A.L.: University of Technology, Department of Chemical and Biological Engineering Polymer Technology, 412 96 Gothenburg, Sweden.

Notes

The authors declare no competing financial interest.

ACKNOWLEDGMENTS

The Danish Council for Independent Research|Natural Sciences (FNU) is thanked for financial support (C.J.M.) and the solid state NMR equipment. U.G.N. acknowledges the "The Danish L'Oréal-UNESCO for Women in Science Fellowship" and "The Villum Young Investigator Programme" for financial support. We are grateful to Professor Gang Wu, Queens University, Canada, for providing the CSA parameters obtained from DFT calculations for the [Al(III)(acac)$_3$] complex.

REFERENCES

(1) Grey, C. P.; Dupre, N. *Chem. Rev.* **2004**, *104*, 4493.

(2) (a) Cole, K. E.; Paik, Y.; Reeder, R. J.; Schoonen, M.; Grey, C. P. *J. Phys. Chem. B* **2004**, *108*, 6938. (b) Kim, J.; Grey, C. P. *Chem. Mater.* **2010**, *22*, 5453. (c) Kim, J.; Li, W.; Philips, B. L.; Grey, C. P. *Energy Environ. Sci.* **2011**, *4*, 4298. (d) Kim, J.; Middlemiss, D. S.; Chernova, N. A.; Zhu, B. Y. X.; Masquelier, C.; Grey, C. P. *J. Am. Chem. Soc.* **2010**, *132*, 16825. (e) Nielsen, U. G.; Heinmaa, I.; Samoson, A.; Majzlan, J.; Grey, C. P. *Chem. Mater.* **2011**, *23*, 3176. (f) Nielsen, U. G.; Majzlan, J.; Grey, C. P. *Chem. Mater.* **2008**, *20*, 2234.

(3) Bakhmutov, V. I. *Chem. Rev.* **2010**, *111*, 530.

(4) Jaroniec, C. P. *Solid State Nucl. Magn. Reson.* **2012**, *43*−*44*, 1.

(5) (a) Ishii, Y.; Wickramasinghe, N. P.; Chimon, S. *J. Am. Chem. Soc.* **2003**, *125*, 3438. (b) Wickramasinghe, N. P.; Kotecha, M.; Samoson, A.; Past, J. *J. Magn. Reson.* **2007**, *184*, 350. (c) Wickramasinghe, N. P.; Parthasarathy, S.; Jones, C. R.; Bhardwaj, C.; Long, F.; Kotecha, M.; Mehboob, S.; Fung, L. W. M.; Past, J.; Samoson, A.; Ishii, Y. *Nat. Methods* **2009**, *6*, 215.

(6) (a) Nielsen, U. G.; Hazell, A.; Skibsted, J.; Jakobsen, H. J.; McKenzie, C. J. *CrystEngComm* **2010**, *12*, 2826. (b) Nielsen, U. G.; Topsøe, N.-Y.; Brorson, M.; Skibsted, J.; Jakobsen, H. J. *J. Am. Chem. Soc.* **2004**, *126*, 4926.
(7) (a) Alberti, E.; Ardizzoia, G. A.; Brenna, S.; Castelli, F.; Galli, S.; Maspero, A. *Polyhedron* **2007**, *26*, 958. (b) Hoser, A. A.; Schilf, W.; Szady Chełmieniecka, A.; Kołodziej, B.; Kamieński, B.; Grech, E.; Woźniak, K. *Polyhedron* **2012**, *31*, 241. (c) Ahmedova, A.; Marinova, P.; Paradowska, K.; Marinov, M.; Wawer, I.; Mitewa, M. *Polyhedron* **2010**, *29*, 1639. (d) Ivanov, A. V.; Bredyuk, O. A.; Antzutkin, O. N.; Forsling, W. *Russ. J. Coord. Chem.* **2004**, *30*, 480. (e) Okazaki, M.; McDowell, C. A. *J. Am. Chem. Soc.* **1984**, *106*, 3185.
(8) Paluch, P.; Potrzebowski, M. J. *Solid State Nucl. Magn. Reson.* **2009**, *36*, 103.
(9) (a) Belle, C.; Bougault, C.; Averbuch, M.-T.; Durif, A.; Pierre, J.-L.; Latour, J.-M.; Le Pape, L. *J. Am. Chem. Soc.* **2001**, *123*, 8053. (b) Roquette, P.; Maronna, A.; Reinmuth, M.; Kaifer, E.; Enders, M.; Himmel, H.-J. *Inorg. Chem.* **2011**, *50*, 1942. (c) Szajna, E.; Dobrowolski, P.; Fuller, A. L.; Arif, A. M.; Berreau, L. M. *Inorg. Chem.* **2004**, *43*, 3988. (d) Yoshida, T.; Kaizaki, S. *Inorg. Chem.* **1999**, *38*, 1054.
(10) (a) Soldatov, D. V.; Diamente, P. R.; Ratcliffe, C. I.; Ripmeester, J. A. *Inorg. Chem.* **2001**, *40*, 5660. (b) Soldatov, D. V.; Henegouwen, A. T.; Enright, G. D.; Ratcliffe, C. I.; Ripmeester, J. A. *Inorg. Chem.* **2001**, *40*, 1626.
(11) (a) Basato, M.; Favero, G.; Veronese, A. C.; Grassi, A. *Inorg. Chem.* **1993**, *32*, 763. (b) Ikeda, R.; Tamura, T.; Yamashita, M. *Chem. Phys. Lett.* **1990**, *173*, 466. (c) Watanabe, R.; Ishiyama, H.; Maruta, G.; Takeda, S. *Polyhedron* **2005**, *24*, 2599.
(12) (a) Lee, H.; Polenova, T.; Beer, R. H.; McDermott, A. E. *J. Am. Chem. Soc.* **1999**, *121*, 6884. (b) Liu, K.; Ryan, D.; Nakanishi, K.; McDermott, A. *J. Am. Chem. Soc.* **1995**, *117*, 6897.
(13) Lee, H.; de Montellano, P. R. O.; McDermott, A. E. *Biochemistry* **1999**, *38*, 10808.
(14) Heise, H.; Köhler, F. H.; Herker, M.; Hiller, W. *J. Am. Chem. Soc.* **2002**, *124*, 10823.
(15) Mizuno, M.; Suzuki, Y.; Endo, K.; Murakami, M.; Tansho, M.; Shimizu, T. *J. Phys. Chem. A* **2007**, *111*, 12954.
(16) Shahid, M.; Hamid, M.; Mazhar, M.; Azad Malik, M.; Raftery, J. *Acta Crystallogr.* **2010**, *E66*, m949.
(17) Charles, R. G.; Pawlikowski, M. A. *J. Phys. Chem.* **1958**, *62*, 440.
(18) Ananikov, V. P.; Gayduk, K. A.; Starikova, Z. A.; Beletskaya, I. P. *Organometallics* **2010**, *29*, 5098.
(19) Porter, L. C.; Dickman, M. H.; Doedens, R. J. *Inorg. Chem.* **1988**, *27*, 1548.
(20) Metin, Ö.; Yildrim, L. T.; Özkar, S. *Inorg. Chem. Commun.* **2007**, *10*, 1121.
(21) Altomare, A.; Cascarano, G.; Giacovazzo, C.; Gualardi, A. *J. Appl. Crystallogr.* **1993**, *26*, 343.
(22) Sheldrick, G. M. *Acta Crystallogr.* **2008**, *A64*, 112.
(23) Farrugia, L. J. J. *Appl. Crystallogr.* **1997**, *30*, 565.
(24) Farrugia, L. J. J. *Appl. Crystallogr.* **1999**, *32*, 837.
(25) Morcombe, C. R.; Zilm, K. W. *J. Magn. Reson.* **2003**, *162*, 479.
(26) Skibsted, J.; Nielsen, N. C.; Bildsøe, H. *J. Magn. Reson.* **1991**, *95*, 88.
(27) Siminovitch, D. J.; Rance, M.; Jeffrey, K. R.; Brown, M. F. *J. Magn. Reson.* **1984**, *58*, 62.
(28) (a) Abernathy, S. M.; Miller, J. C.; Lohr, L. L.; Sharp, R. R. *J. Chem. Phys.* **1998**, *109*, 4035. (b) Kurland, R. J.; McGarvey, B. R. *J. Magn. Reson.* **1970**, *2*, 286. (c) Abernathy, S. M.; Sharp, R. R. *J. Phys. Chem. A* **1997**, *101*, 3692.
(29) Bullen, G. J.; Mason, R.; Pauling, P. *Inorg. Chem.* **1965**, *4*, 456.
(30) Ley, H. *Ber. Dtsch. Chem. Ges.* **1914**, *47*, 2948.
(31) Montgomery, H.; Lingafelter, E. C. *Acta Crystallogr.* **1964**, *17*, 1481.
(32) Zhou, X.-F.; Han, A.-J.; Chu, D.-B.; Huang, Z.-X. *Acta Crystallogr.* **2001**, *57*, m506.
(33) Wong, A.; Smith, M. E.; Terskikh, V.; Wu, G. *Can. J. Chem.* **2011**, *89*, 1087.
(34) Wu, G., Personal communication. 2012.
(35) Shibata, S.; Kishita, M.; Kubo, M. *Nature* **1957**, 179.
(36) Hursthouse, M. B.; Laffey, M. A.; Moore, P. T.; New, D. B.; Raithby, P. R.; Thornton, P. *J. Chem. Soc., Dalton Trans.* **1982**, *2*, 307.
(37) Jensen, T. R.; McGinley, J.; McGee, V.; McKenzie, C. *J. Acta Chem. Scand.* **1998**, *52*, 622.
(38) Romero, R. R.; Cervanteslee, F.; Porter, L. C. *Acta Crystallogr.* **1992**, *C48*, 993.
(39) Spiess, H. W. *NMR* **1978**, *15*, 55.
(40) Romero, R. R.; Cervantes-Lee, F.; Porter, L. C. *Acta Crystallogr.* **1992**, *C48*, 993.
(41) Miller, J.; Abernathy, S.; Sharp, R. *J. Phys. Chem. A* **2000**, *104*, 4839.
(42) Ryan, D. E.; Nakanishi, K. *J. Labelled Compd. Radiopharm.* **1995**, *36*, 595.